Cold Crystallization of PDMS and PLLA in Poly(L - lactide - b - dimethylsiloxane - b - L - lactide) Triblock Copolymer and Their E ff ect on Nanostructure Morphology

DATASET · AUGUST 2015

Macromolecules

Article

pubs.acs.org/Macromolecules

Cold Crystallization of PDMS and PLLA in Poly(L-lactide-*b*-dimethylsiloxane-*b*-L-lactide) Triblock Copolymer and Their Effect on Nanostructure Morphology

S. Nagarajan and E. Bhoje Gowd*

Materials Science and Technology Division, CSIR-National Institute for Interdisciplinary Science and Technology, Trivandrum 695 019 Kerala, India

Supporting Information

ABSTRACT: Poly(L-lactide-*b*-dimethylsiloxane-*b*-L-lactide) (PLLA-*b*-PDMS-*b*-PLLA) triblock copolymer was synthesized by ring-opening polymerization of L-lactide using bis-(hydroxyalkyl)-terminated PDMS as a macroinitiator. The block copolymer was immiscible in the melt, and the melt morphology was preserved upon cooling the melt to −120 °C. It was also observed that at moderate cooling rates PDMS and PLLA blocks remain in the amorphous phase at temperatures below −120 °C. The breakout and preservation of the nanostructure morphology of the triblock copolymer have been investigated by variable temperature small-angle and wide-angle X-ray scattering (SAXS and WAXS) during heating. The crystallization and melting of PDMS block occurred within the confined space entrenched by the amorphous PLLA block in the temperature range from −120 to 40 °C by preserving the microphase-separated morphology. At around the glass transition temperature of PLLA (∼45 °C), chain stretching of PLLA and PDMS took place, resulting in the sudden increase of the lamellar long period. In this temperature region, amorphous PLLA transiently transformed to the mesophase structure that resulted in the increase of PLLA domain thickness. At higher temperature, the morphological perturbation was induced by the breakout crystallization of PLLA block. In addition, the effect of isothermal cold crystallization temperatures on the polymorphic behavior of PLLA in PLLA-*b*-PDMS-*b*-PLLA triblock copolymers was also investigated. It was found that the polymorphic behavior of PLLA was not influenced much by the presence of PDMS blocks. The disordered (α') and ordered (α) forms are formed at low and high cold crystallization temperatures, respectively, similar to the PLLA homopolymer.

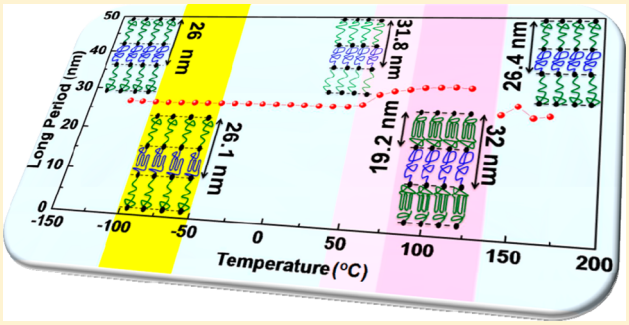

INTRODUCTION

Poly(L-lactide) (PLLA) is one of the most popular biodegradable and biocompatible polymers.[1−4] It has been widely used in the industrial and medical fields, for example, sutures, scaffolds, and orthopedic fixation devices because of its high strength, high modulus, and biocompatibility.[5−8] PLLA exhibits polymorphic behavior depending upon the application of external stimuli such as temperature, solvent atmosphere, etc.[9−12] PLLA crystallizes into α, β, γ, δ (α'), and ε polymorphic forms.[9,12−19] The most stable crystalline form of PLLA is α form. Each crystalline form was found to have different sets of properties, and therefore, this material can be used for various applications.[20,21] Extensive studies have been carried out to understand the relation between crystalline structure and processing condition for tailoring the physical performance of the PLLA homopolymers. Recently, synthesis of PLLA containing block copolymers has attracted great interest from a number of researchers because of their applications in the medical field and nanolithography.[22−27] In reminding the importance of PLLA, herein, we have synthesized poly(L-lactide-*b*-dimethylsiloxane-*b*-L-lactide) (PLLA-*b*-PDMS-*b*-PLLA) triblock copolymers. The incorporation of PDMS segments into block copolymers is highly attractive since PDMS containing block copolymers can be used as multifunctional materials for nanolithographic applications.[26] PDMS containing block copolymers are promising materials for pattern transfers due to its high etch contrast from the high silicon density in PDMS.[23,28] Although some groups have studied the crystallization behavior of crystalline−crystalline block copolymers, the structural formation of double crystalline block copolymers remains largely unresolved.

Crystallization in block copolymers is a very interesting subject and attracted much attention in the past few decades.[24,29−31] The introduction of crystallizable blocks in block copolymers controls the solid state structure and generates fascinating morphologies due to the complex interplay between microphase separation and crystallization.[32,33] The segregation strength of the blocks in the melt state determines the morphological development in the crystalline block copolymers, which is controlled by two

Received: June 1, 2015
Revised: June 22, 2015
Published: July 27, 2015

DOI: 10.1021/acs.macromol.5b01179
Macromolecules 2015, 48, 5367−5377

competing self-organizing mechanisms, namely, microphase separation and crystallization. For example, for strongly segregated melts, crystallization will be confined within the block copolymer microdomains and for weakly segregated melts; the crystallization can overwrite the preformed structure. The simplest and most studied crystallizable block copolymers are crystalline−amorphous diblock copolymers where one of the blocks can crystallize while other remains amorphous.[30,31,34,35] The final morphology formed by such crystalline−amorphous block copolymers depends upon the relative location of the transition temperatures, i.e., the order−disorder temperature (T_{ODT}), the crystallization temperature (T_c), and the glass transition temperature of the amorphous block (T_g).[36−42]

In block copolymers containing only crystallizable blocks, the situation is more complicated because of the competition between the crystallization of different crystalline blocks. The crystallization of one block may affect the crystallization and morphology of the other block. The crystallization behavior of several crystalline−crystalline (di- and triblock) copolymers has been studied.[24,25,43,44] It has been reported that if the melting temperatures for both blocks in a double-crystalline polymer are similar, both blocks can crystallize together from the melt for symmetric block ratios. As a consequence, the final morphologies of the block copolymer are more complicated due to the interactive effect of the microphase separation, crystallization, vitrification, and sequence of crystallization.[45,46] On the contrary, if the melting temperatures for both blocks in a double-crystalline polymer are far from each other, the crystallization temperatures of both blocks are comparable to that of the corresponding homopolymers. A difference in the crystallization temperatures of both blocks may result in the fractioned crystallization as a consequence of the confined crystallization of the lower temperature block.[47,48] Depending on the mechanical strength of the template, various final morphologies are possible. For a vigorous crystalline template, the final morphology of the block copolymer will be dictated by previously crystallized block.[47,49−53] In contrast, for a wobbly crystalline template, the subsequent crystallization may devastate the established crystalline morphology, triggering a morphological transition.[54,55]

Here, we have chosen poly(L-lactide-*b*-dimethylsiloxane-*b*-L-lactide) (PLLA-*b*-PDMS-*b*-PLLA) triblock copolymer, where the melting temperatures of both blocks are far from each other. This polymer is a typical example of the amorphous−crystalline triblock copolymer at room temperature. However, when the copolymer cooled to subambient temperature, it behaves as a double crystalline triblock copolymer. It was observed that at moderate cooling rates PDMS and PLLA blocks in triblock copolymer did not crystallize, and it remains in the amorphous phase at temperatures around −120 °C. PDMS and PLLA are reported to be immiscible in melt and on cooling triblock copolymer showed a microphase separation.[22,26] On subsequent heating, both PDMS and PLLA were found to crystallize, and it enables us to investigate the cold crystallization of both blocks and its influence on the block copolymer nanostructure. To the best of our knowledge, most previous studies on crystalline−crystalline block copolymers have reported the change in morphology upon crystallization induced by stepwise cooling or at a given temperature. For the first time, we have investigated the morphological changes during the cold crystallization of components on heating of the amorphous triblock copolymer. In addition, very limited studies have been focused on the crystallization behavior of PDMS in block copolymers. In this work, the nanostructure morphology of a double crystalline triblock copolymer was investigated as a function of temperature using small-angle and wide-angle X-ray scattering (SAXS and WAXS). In addition, the effect of isothermal cold crystallization temperatures on the polymorphic behavior of PLLA was also investigated.

EXPERIMENTAL SECTION

Materials. L-Lactide, bis(hydroxyalkyl)-terminated poly(dimethylsiloxane) ($\bar{M}_n$ = 5600), tin(II) 2-ethylhexanote Sn(Oct)$_2$, dry toluene, and hexane were purchased from Sigma-Aldrich. The chemicals were used as received without further purification.

Synthesis of PLLA-*b*-PDMS-*b*-PLLA. In a typical procedure, 1 g of bis(hydroxyalkyl)-terminated poly(dimethylsiloxane) ($\bar{M}_n$ = 5600 g/mol) and 5 mg of Sn(Oct)$_2$ were added to a dried round-bottom flask containing dry toluene (50 mL). The solution was stirred under a nitrogen atmosphere for 30 min at 60 °C. 2 g of L-lactide was added to the stirring mixture slowly, and the temperature was raised to 115 °C. After approximately 72 h at 115 °C, the solution was cooled down to room temperature. The polymer was separated and purified by precipitation with 500 mL of cold hexane twice. The filtered polymer was dried at 60 °C under vacuum for 48 h. The number-average molecular weight and polydispersity of the PLLA-*b*-PDMS-*b*-PLLA triblock copolymer estimated to be $\bar{M}_n$ = 19 300 g/mol and $\bar{M}_w/\bar{M}_n$ = 1.3, respectively. Homopolymer of PLLA was synthesized using the similar procedure without adding PDMS.

Preparation of PLLA and PDMS Homopolymer Blends. Homopolymer blends of PLLA ($\bar{M}_n$ = 22 500 g/mol; $\bar{M}_w/\bar{M}_n$ =1.24) and PDMS ($\bar{M}_n$ = 5600 g/mol) were prepared by solution blending method. 1:1 weight ratio of homopolymers was dissolved in chloroform, and the solution was casted into films. The solvent was allowed to evaporate under ambient conditions, and the blend was subsequently dried in vacuum at 60 °C for 1 h.

Characterization. *X-ray Diffraction Measurements.* Wide-angle and small-angle X-ray scattering measurements were carried out on XEUSS SAXS/WAXS system using a Genixmicro source from Xenocs operated at 50 kV and 0.6 mA. The Cu Kα radiation (λ = 1.54 Å) was collimated with FOX2D mirror and two pairs of scatterless slits from Xenocs. The 2D-patterns were recorded on a Mar345 image plate and processed using Fit2D software. These measurements were made in the transmission mode. Silver behenate and silicon powder were used as standard materials for calibration of the scattering vectors of SAXS and WAXS, respectively. Mar 345 dtb image plate detector was set at 1050 mm and 221.75 mm from the sample in the direction of the beam for SAXS and WAXS data collections, respectively. The XEUSS SAXS/WAXS system is equipped with a Linkam THMS 600 hot stage and a Linkam TMS 93 programmable temperature controller. The Linkam hot stage was connected to the LNP 95 cooling system, which cools the stage to liquid nitrogen temperature. The flow of nitrogen was automatically adjusted with the help of T95 controller.

Differential Scanning Calorimetry (DSC). The crystallization and melting behavior of triblock copolymer were measured using a differential scanning calorimeter (PerkinElmer Pyris 6 DSC). Samples of approximately 8 mg were encapsulated in aluminum pans. The calibration was performed with indium, and all the DSC experiments were conducted under a nitrogen atmosphere. The thermal program employed for the isothermal crystallization of PLLA is depicted in Figure S1. A sample was heated from room temperature to 190 °C (above melting temperature of PLLA) at a rate of 10 °C/min, where it was held for 2 min to erase the thermal history of the sample, and then cooled to 0 °C at a rate of 50 °C/min. In the second heating, the sample was heated to a desired crystallization temperature (T_c) at a rate of 50 °C/min and kept for 1 h for the isothermal crystallization.

Nuclear Magnetic Resonance Spectroscopy (NMR). The structure of triblock copolymer was confirmed by ^{1}H NMR ($CDCl_3$ solvent) using a Bruker NMR spectrometer operating at 500 MHz. The number-average molecular weight of the triblock copolymer was estimated based on the integrated values of ^{1}H NMR peaks.[22]

DOI: 10.1021/acs.macromol.5b01179
Macromolecules 2015, 48, 5367−5377

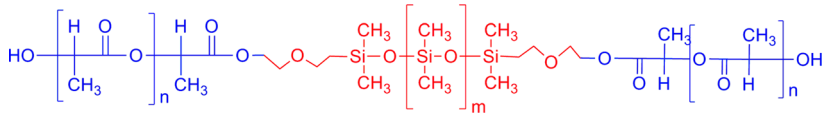

Figure 1. Chemical structure of PLLA-*b*-PDMS-*b*-PLLA triblock copolymer.

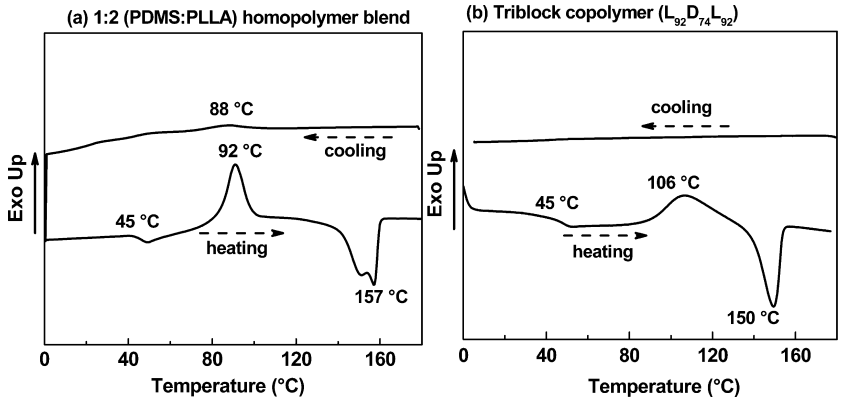

Figure 2. DSC cooling (upper) and reheating thermograms obtained at a rate of 10 °C/min: (a) PDMS:PLLA homopolymer blend and (b) PLLA-*b*-PDMS-*b*-PLLA triblock copolymer ($L_{92}D_{74}L_{92}$).

Gel Permeation Chromatography (GPC). Molecular weight distribution profiles were determined by GPC at room temperature using an Agilent Technologies-1260 instrument equipped with a PL-gel 20 μm MIXED-B column and RI detector. Polymers were injected (50 μL) into the column as solutions in THF (5 mg/mL) with a flow rate of 1 mL/min. The molecular weight was measured relative to polystyrene according to universal calibration using narrow disperse standards.

Fourier Transform Infrared Spectroscopy (FTIR). The infrared spectra were measured with a PerkinElmer series Spectrum Two FT-IR spectrometer over the wavenumber range of 4000−400 cm^{-1}. The powder sample was mixed with potassium bromide (KBr) powder and pressed in the form of pellets for FTIR measurements. The FTIR spectra were collected with 32 scans and a resolution of 2 cm^{-1}. The variable temperature infrared spectra were collected using the same hot stage used for the X-ray measurements.

RESULTS AND DISCUSSION

Synthesis and Characterization of PLLA-*b*-PDMS-*b*-PLLA. PLLA-*b*-PDMS-*b*-PLLA triblock copolymer was synthesized by ring-opening polymerization of L-lactide using $Sn(Oct)_2$ as the initiator and bis(hydroxyalkyl)-terminated poly(dimethylsiloxane) as the macroinitiator.[27] The chemical structure of the PLLA-*b*-PDMS-*b*-PLLA triblock copolymer is shown in Figure 1. The structure of the synthesized block copolymers was confirmed by ^1H NMR (Figure S2). The structural analysis from GPC and NMR determines that the molecular weight and polydispersity of the PLLA-*b*-PDMS-*b*-PLLA triblock copolymer are $\bar{M}_n$ = 19 300 g/mol and $\bar{M}_w/\bar{M}_n$ = 1.3, respectively.[22]

Figure 2 shows the DSC cooling and subsequent heating curves collected at 10 °C/min for the homopolymer blend and triblock copolymer ($L_{92}D_{74}L_{92}$). Upon cooling, an exothermic peak was observed at 88 °C for the homopolymer blend corresponding to the melt crystallization of PLLA, and on subsequent heating several transition temperatures were found. The T_g of the PLLA in the homopolymer blend is located at 45 °C, which is almost identical to that of the PLLA homopolymer indicating the immiscible nature of PLLA and PDMS. On further heating, the blended sample showed an exothermic peak at 92 °C corresponding to the cold crystallization of PLLA. That means some fraction of the PLLA was crystallized during cooling from the melt, and on subsequent heating, most of the PLLA crystallizes. The transition temperatures (glass transition, crystallization, and melting) of PDMS are outside the temperature range of the cooling device used with the DSC instrument in our laboratory.

On the other hand, no crystallization peak was detected in the cooling curve of the triblock copolymer ($L_{92}D_{74}L_{92}$). That means the crystallization of PLLA block is strongly retarded during the cooling process at 10 °C/min in triblock copolymer compared to that of the physical blend. Many authors studied the crystallization behavior of PLLA containing block copolymers. However, such retardation of PLLA crystallization on cooling was not reported.[22,25,48,49,56] It is worth mentioning here that Müller and co-workers reported the delay of PLLA crystallization during the cooling process (from the melt) in polyethylene-*b*-poly(L-lactide) (PE-*b*-PLLA).[56] They reported the coincident crystallization of PLLA block with PE block at lower temperatures during the cooling process. On subsequent heating of the triblock copolymer, three transition temperatures; i.e., glass transition temperature (T_g), cold crystallization temperature (T_{cc}), and melting temperature (T_m) were observed at 45, 106, and 150 °C, respectively. These transition temperatures are corresponding to PLLA block in the triblock copolymer. To the best of our knowledge, this type of cold crystallization behavior and its influence on the nanostructure has not been reported earlier for PLLA containing block copolymers. PDMS crystallizes readily at lower temperatures because of its molecular symmetry and small side groups.[57] Our DSC experiments did not reveal any information about the crystallization and melting behavior of PDMS in the triblock copolymer. Only a few studies have described the PDMS crystallization behavior in block copolymers.[57−59] As for the literature, the glass transition temperature, crystallization temperature, and melting temperature of PDMS homopolymer with the typical molecular weights are −125, −90, and −40 °C, respectively.[58,59]

In order to confirm the transition temperatures of PDMS used in this study, wide-angle X-ray diffraction patterns were

DOI: 10.1021/acs.macromol.5b01179
Macromolecules 2015, 48, 5367−5377

collected as a function of temperature during heating of amorphous PDMS (see Supporting Information Figure S3). The cold crystallization temperature and the melting temperature of PDMS measured in this study are in good agreement with the literature values.[58,59]

Melt Structure of Triblock Copolymer. Melt structure of the triblock copolymer ($L_{92}D_{74}L_{92}$) was investigated by SAXS. Figure 3 shows the Lorentz-corrected SAXS profile of triblock copolymer collected at 170 °C (melt state). The SAXS pattern exhibits two reflections at relative q values of 1:2, suggesting the formation of microphase-separated lamellar morphology with the interlamellar distance (calculated from the primary reflection) of 26.4 nm in the melt state. The existence of the microphase-separated lamellar morphology in the melt state was attributed to the strong segregation of the PLLA and PDMS blocks. The significant difference between the Hildebrand solubility parameters of PLLA (δ_{PLLA} = 19.8 $MPa^{1/2}$) and PDMS (δ_{PDMS} = 15.1 $MPa^{1/2}$) also suggested the incompatibility between PLLA and PDMS blocks.[26,27] On the other hand, the homopolymer blend sample did not show any reflections in SAXS profile due to the macrophase separation between PLLA and PDMS.

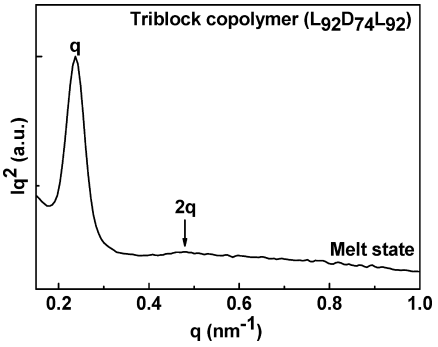

Figure 3. Lorentz-corrected SAXS profile of PLLA-*b*-PDMS-*b*-PLLA triblock copolymer melt at 170 °C.

Effect of Cold Crystallization on Microphase-Separated Morphology. The triblock copolymer ($L_{92}D_{74}L_{92}$) melt was cooled to −120 °C at 30 °C/min in a Linkam hot stage connected to the LNP 95 cooling system. The WAXS pattern reveals a broad amorphous halo at −120 °C (Figure 4a), indicating that no crystallization of PLLA and PDMS occurred in the triblock copolymer ($L_{92}D_{74}L_{92}$) after cooling from the melt. The corresponding SAXS pattern looks almost similar to the SAXS pattern of triblock copolymer ($L_{92}D_{74}L_{92}$) melt with the reduced intensity. The melt and the solidified triblock copolymer (at −120 °C) exhibit the same q value at ∼0.24 nm^{-1}, indicating that the melt microphase-separated lamellar morphology was preserved upon cooling to −120 °C. To further understand the relationship between the crystallization of both the blocks and their influence on the microphase-separated structure, temperature-dependent WAXS and SAXS patterns of amorphous triblock copolymer were measured.

Figure 4 shows the temperature-dependent WAXS and SAXS patterns during the heating process (at 10 °C/min) from −120 to 170 °C. The temperature dependence of the integrated intensities of X-ray reflections corresponding to PDMS and PLLA is shown in Figure 5. Upon heating, WAXS results (Figure 4a) revealed that the onset of PDMS crystallization in triblock copolymer is evidenced at −110 °C by the appearance

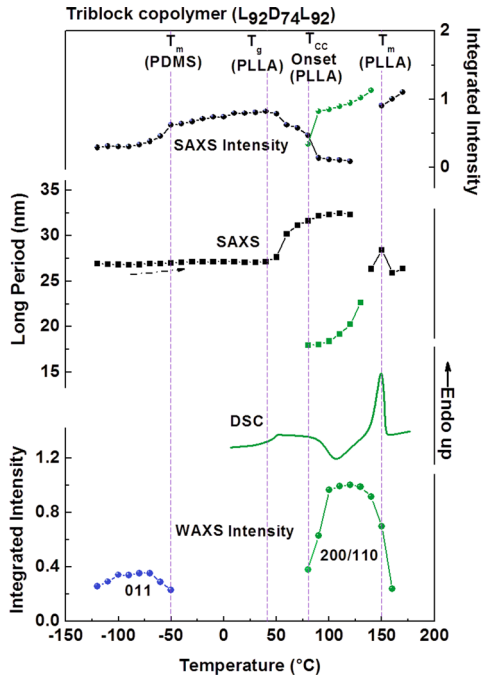

Figure 5. Comparison of the SAXS intensity, long period, DSC heating curve (from 0 to 170 °C), and the WAXS intensities of 011 reflection of PDMS and 200/110 reflection of PLLA during the heating process of the amorphous PLLA-*b*-PDMS-*b*-PLLA triblock copolymer from −120 to 170 °C.

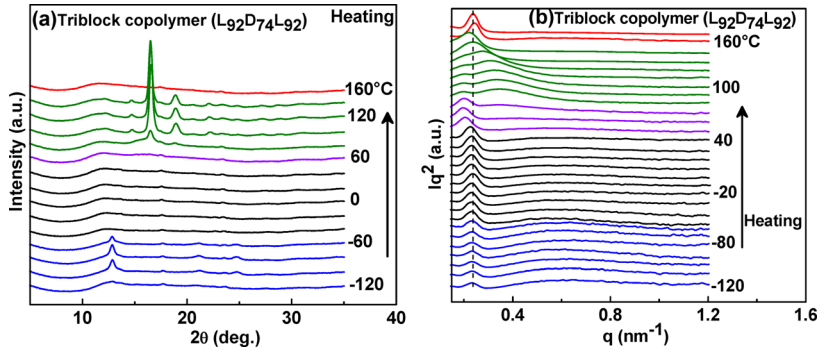

Figure 4. (a) WAXS patterns and (b) SAXS patterns (Lorentz-corrected) measured during heating of the amorphous PLLA-*b*-PDMS-*b*-PLLA triblock copolymer from −120 to 170 °C.

DOI: 10.1021/acs.macromol.5b01179
Macromolecules 2015, 48, 5367−5377

of X-ray peaks at 2θ = 12.9° (011), 21.2° (020), and 24.8° (121/013). On further heating, as seen in Figure 5, the intensity of the 011 reflection increased and reached its maximum at −70 °C. At −50 °C, the intensity of the 011 reflection decreased due to the melting of PDMS crystals. The onset of cold crystallization temperature of PDMS in the triblock copolymer decreased notably (from −90 to −110 °C) in comparison with its PDMS homopolymer (Figure S3). The decreased cold crystallization temperature indicates the enhanced crystallization rate of PDMS in the triblock copolymer, which may be interpreted as a nucleation effect caused by the PLLA block. The corresponding SAXS patterns did not show any obvious change in this temperature range as seen in Figure 4b other than the increase in intensity of the SAXS peak at around PDMS melting. The temperature dependence of the long period and the intensity changes estimated from the SAXS patterns are depicted in Figure 5. The unchanged SAXS patterns (long period values) in the temperature range from −120 to −70 °C indicate the preservation of microphase-separated morphology during crystallization of PDMS. These results suggested that the amorphous PLLA block created a hard template similar to the hard confinement for the PDMS crystallization, and no dimensional change in the self-assembled morphologies was observed. At around −40 °C, X-ray peaks corresponding to the PDMS crystals disappeared completely, indicating the melting of PDMS. The corresponding SAXS patterns remain unchanged after PDMS melting, indicating that the PDMS melting was confined within the amorphous PLLA blocks. In the temperature range from −40 to 40 °C, both PDMS and PLLA blocks remain in the amorphous phase. No obvious changes were observed both in WAXS and SAXS patterns other than the increase in the intensity of the SAXS peak. Such an increase in the intensity of the SAXS peak may be interpreted as the result of the enhanced electron density contrast between the amorphous PLLA and amorphous PDMS due to the melting of PDMS block.

In order to estimate the thickness of the PLLA and PDMS microdomains, we analyzed the SAXS data by calculating the one-dimensional electron density correlation function curves. Details on the one-dimensional electron density correlation function calculations can be found in the Supporting Information. The one-dimensional electron density correlation function ($K(z)$) curves derived from the scattering curves at three different temperatures (−120, 70, and 100 °C) in the heating process are shown in Figure 6. The long period was calculated from the first maxima in the correlation curve based on the method described in the literature.[60−62] The intercept of the tangent of the correlation curve and the horizontal line of the first minima (as shown in Figure 6) provide an estimate of the thickness of thinner layer. Since the volume fraction of PDMS blocks in the PLLA-*b*-PDMS-*b*-PLLA triblock copolymer was small, we would attribute the thinner spacing to PDMS microdomain. The long period and respective domain sizes of PLLA and PDMS blocks estimated from $K(z)$ curves are plotted as a function of temperature as shown in Figure 7. At −120 °C, the long period was calculated to be 26 nm, which consisted of 8.3 nm thick PDMS layer and 17.7 nm thick PLLA layer (Figure 6a). In the temperature range from −120 to 40 °C, no obvious changes were observed in both long period and PLLA domain thickness other than a slight increase in the thickness of the PDMS microdomain due to the melting of PDMS block at around −50 °C as shown in Figure 7.

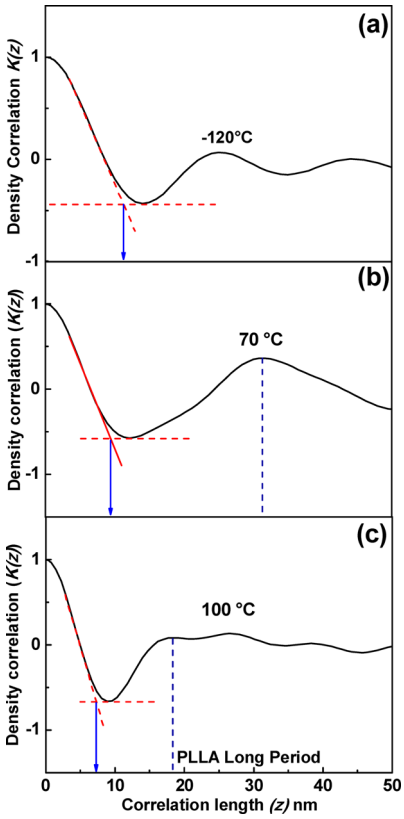

Figure 6. One-dimensional electron density correlation function calculated based on the SAXS data of PLLA-*b*-PDMS-*b*-PLLA triblock copolymer in the heating process: (a) −120, (b) 70, and (c) 100 °C.

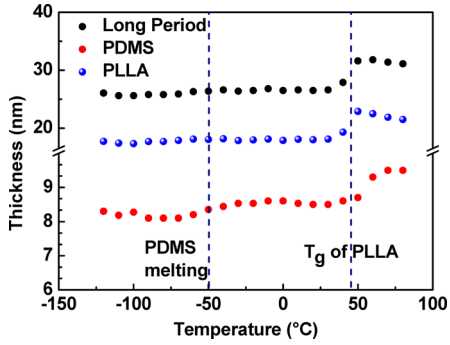

Figure 7. Temperature-dependent long periods and respective domain sizes of PLLA and PDMS blocks determined by one-dimensional electron density correlation function.

On further heating, the long period values estimated from the primary reflection of SAXS pattern increased dramatically at around 50 °C (Figures 5 and 7). Figure 6b shows the one-dimensional correlation function of the triblock copolymer at 70 °C. The $K(z)$ curve estimated at 70 °C showed some distortion in shape, which might be due to the formation of PLLA mesophase in triblock copolymer at 70 °C (see below for further discussion). In a more recent study, Hawker and co-workers also reported such distorted $K(z)$ curves in poly(propylene oxide)-*b*-poly(ethylene oxide)-*b*- poly(propylene oxide) triblock copolymers due to the crystallization of one of the blocks.[63] The long period, the PDMS thickness, and PLLA thickness were determined as 31.5, 9.6, and 21.9 nm. The long period value estimated from the $K(z)$ curve was in good agreement with the long period obtained by Bragg's law from

DOI: 10.1021/acs.macromol.5b01179
Macromolecules 2015, 48, 5367−5377

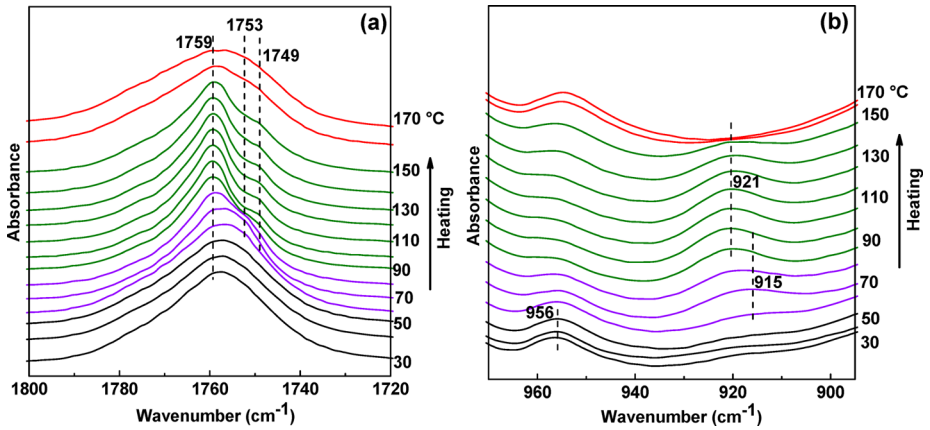

Figure 8. Temperature-dependent infrared spectra of amorphous PLLA-*b*-PDMS-*b*-PLLA triblock copolymer measured during heating process from 30 to 170 °C in the frequency region of (a) C═O stretching vibration and (b) C−C backbone vibration.

the SAXS pattern at 70 °C (32 nm). The DSC heating curve shown in Figure 5 displayed that the glass transition temperature of PLLA in the triblock copolymer was around 45 °C. It means at around the glass transition temperature of PLLA block a sudden increase in the thickness of PDMS and PLLA microdomains was observed. On the basis of the experimental results, it is reasonable to suggest that the molten PDMS chains, which are confined within the PLLA microdomains, were stretched as a result of segmental mobility of the PLLA chains at around its glass transition temperature. This situation may have resulted in the increase of PDMS microdomain thickness. On the other hand, we might have two possibilities to explain the increase of PLLA microdomain thickness. For example, we may speculate that the mobility of PLLA chains in the copolymer is enhanced in the presence of molten PDMS chains above the glass transition temperature of PLLA. In this situation, the thermal motions of the chains may lead to the free volume expansion, and as a result, the microdomain thickness of the amorphous PLLA might have increased above the glass transition temperature. Another possibility is the formation of mesophase of PLLA in the triblock copolymer just above the glass transition temperature. The shape of the amorphous halo in the corresponding WAXS patterns confirms the formation of PLLA mesophase in triblock copolymer just above the glass transition temperature. In order to further confirm the formation of PLLA mesophase, temperature-dependent infrared spectra of amorphous PLLA-*b*-PDMS-*b*-PLLA triblock copolymer were measured during the heating process as shown in Figure 8. The PDMS block in PLLA-*b*-PDMS-*b*-PLLA triblock copolymer lacks the C−C backbone and C═O groups; hence, the spectral regions of C═O stretching vibration and C−C backbone vibration are dominated by the signals of PLLA. As seen in Figure 8, obvious spectral differences are observed in the C═O stretching vibration region (Figure 8a) and C−C backbone vibration region (Figure 8b). Meaurio et al.[64,65] showed that the IR bands in the C═O stretching region are sensitive to the chain conformations and the bands at 1777, 1767, 1759, and 1749 cm^{-1} are assigned to gg, gt, tg, and tt conformers, respectively. As shown in Figure 8a, no spectral splitting is observed at 30 °C for the quenched PLLA-*b*-PDMS-*b*-PLLA triblock copolymer. The IR band located at 1757 cm^{-1} is assigned to the amorphous phase of PLLA.[64] However, when the sample is heated to a temperature above 50 °C, a new band appeared at 1753 cm^{-1}. Zhang et al.[66] observed this band in the melt quenched poly(L-lactide-*b*-ethylene glycol-*b*-L-lactide) (PLLA-*b*-PEG-*b*-PLLA) triblock copolymer and was assigned to the mesophase of PLLA. At this temperature, PLLA in triblock copolymer seems to be an intermediate state between crystalline and amorphous phase. The appearance of IR band at 1753 cm^{-1} may suggest an increase of the tt conformers above 50 °C. On further heating, at around 90 °C, the band (1753 cm^{-1}) corresponding to the mesophase disappeared, and a new band appeared at 1749 cm^{-1}. At the same temperature, the band at 1757 cm^{-1} shifted to 1759 cm^{-1}. The appearance of new bands at 1749 and 1759 cm^{-1} indicated the transformation of mesophase into the α crystalline form at around 90 °C. The appearance and disappearance of mesophase of PLLA were also seen in the C−C backbone vibration region. As shown in Figure 8b, the band corresponding to the mesophase at 915 cm^{-1} appeared in the temperature range of 60−80 °C, and on further heating the band corresponding to the α crystalline form appeared at 90 °C.[66] The FTIR results confirmed that the amorphous PLLA in triblock copolymer transiently transforms to the mesophase before transforming into the stable α crystalline form. On the basis of these results, we may say that the sudden increase in the PLLA microdomain thickness at around the glass transition temperature of PLLA might be due to the formation of mesophase, where the relative population of tt conformers is more compared to the amorphous phase or α crystalline form of PLLA.

On further heating, the crystallization of PLLA block occurred in a broad temperature range from 70 to 130 °C as evidenced by the WAXS profiles and DSC thermogram. The WAXS results revealed that the onset of PLLA crystallization is displayed at 70 °C. On heating, well-defined X-ray peaks appeared at 2θ = 14.8° (010), 16.5° (110/200), 18.9° (203), 20.7° (204), 22.3° (015), 24.6°, and 27.3° (207). The presence of X-ray peak at 24.6° suggests that the PLLA in triblock copolymer crystallized into the mixture of α' and α forms.[13,22] It has been reported that the α' form is formed when the PLLA homopolymer was crystallized at temperatures lower than 100 °C.[13−15] When PLLA was crystallized in the temperature region of 100−120 °C, mixtures of α' and α forms are formed. At higher crystallization temperature above 120 °C, PLLA α form is formed. In our case, as evidenced from the DSC, the sample was crystallized at 106 °C and as a result PLLA was crystallized into the mixture of α' and α forms in the triblock copolymer. At the same time, significant changes were observed in the corresponding SAXS patterns when the PLLA block was

DOI: 10.1021/acs.macromol.5b01179
Macromolecules 2015, 48, 5367−5377

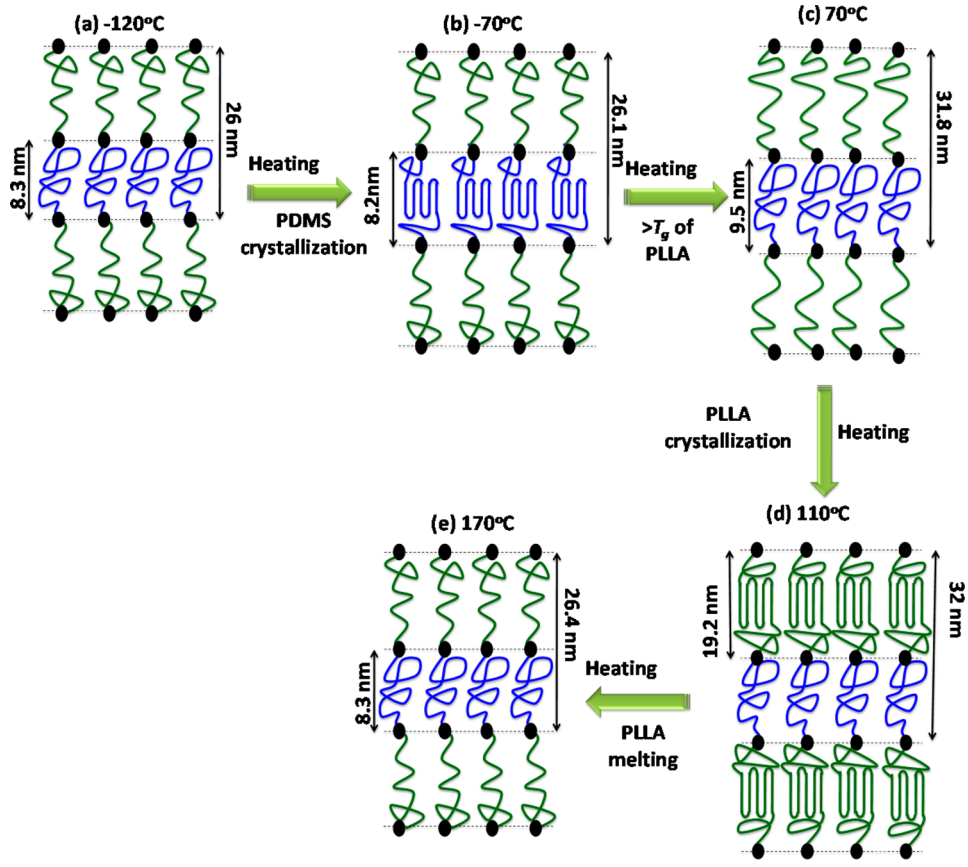

Figure 9. Schematic representation of nanostructure morphologies formed during heating of the amorphous PLLA-*b*-PDMS-*b*-PLLA triblock copolymer from −120 to 170 °C: (a) amorphous triblock copolymer at −120 °C, (b) crystalline PDMS-amorphous PLLA at −70 °C, (c) amorphous PDMS-amorphous PLLA at 70 °C (just above T_g of PLLA), (d) amorphous PDMS-crystalline PLLA at 110 °C and (e) melt at 170 °C. The figure is not to scale.

crystallized. The intensity of the SAXS reflection at q_1 = 0.20 nm^{-1} (L_1 = 32 nm) drastically reduced, and simultaneously a new broad reflection is appeared at q_2 = 0.33 nm^{-1} (L_2 = 19.2 nm). It means that the new peak appeared is due to the lamellar structure of crystallized PLLA. At this temperature, PLLA crystallization took place in the lamellar microdomains surrounded by the soft PDMS phase. In this situation, PLLA-*b*-PDMS-*b*-PLLA triblock copolymer is a crystalline−amorphous system, and the crystallization of PLLA block could perturb the microphase separation. This type of perturbation might be due to the breakout of the microdomain structure to form crystalline lamellar morphology of PLLA or local distortion of the lamellar microdomains. The one-dimensional correlation function estimated in this temperature range (at 100 °C) displays a complex shape due to the overlap of two periodic structures, i.e., semicrystalline PLLA structure and the locally distorted lamellar microdomain structure (Figure 6c). Han and co-workers showed two different periodic structures in crystalline−crystalline block copolymers using the one-dimensional correlation function.[50] As the segregation strength between PLLA and PDMS is very strong, the breakout of the microdomain is more difficult and more distorted microdomains are possible. A similar kind of observation has been reported for crystalline−amorphous diblock copolymers.[24,67] At around 150−160 °C, as evidenced by DSC and WAXS, the PLLA crystals melt. At this temperature, a drastic change in the SAXS pattern was observed. The SAXS peak corresponding to the melt structure appeared at q = 0.24 nm^{-1} (L = 26.4 nm) along with the second-order reflection at q = 0.48 nm^{-1}, suggesting the formation of a microphase-separated lamellar morphology of triblock copolymer in the melt state.

By combining the WAXS, SAXS, and DSC results, we suggested a model to explain the structural changes for self-assembled morphologies formed by the amorphous PLLA-*b*-PDMS-*b*-PLLA triblock copolymer during the heating process as schematically illustrated in Figure 9. At −120 °C, PDMS and PLLA chains both exhibited the random coiled chain conformations and strongly segregated to form the microphase-separated lamellar morphology with the long period value around 26 nm (Figure 9a). The PDMS block crystallized first within the template created by amorphous PLLA block in the temperature range from −120 to −70 °C by preserving the microphase-separated morphology (Figure 9b). On further heating, at around −50 °C, PDMS melts within the hard template of PLLA. The unchanged SAXS patterns (long period values) in the temperature range from −120 to 40 °C indicate the preservation of microphase-separated morphology during crystallization and melting of PDMS. This indicated that the crystallization and melting of PDMS block progressed within the confined space entrenched by the amorphous PLLA block. However, when the temperature reached the glass transition temperature of PLLA (~45 °C), a sudden increase in the long period values (from 26 to 32 nm) was observed due to the increase in the domain thickness of both PLLA and PDMS microdomains (Figure 9c). The WAXS and DSC results revealed that the crystallization of PLLA had not occurred in

DOI: 10.1021/acs.macromol.5b01179
Macromolecules 2015, 48, 5367−5377

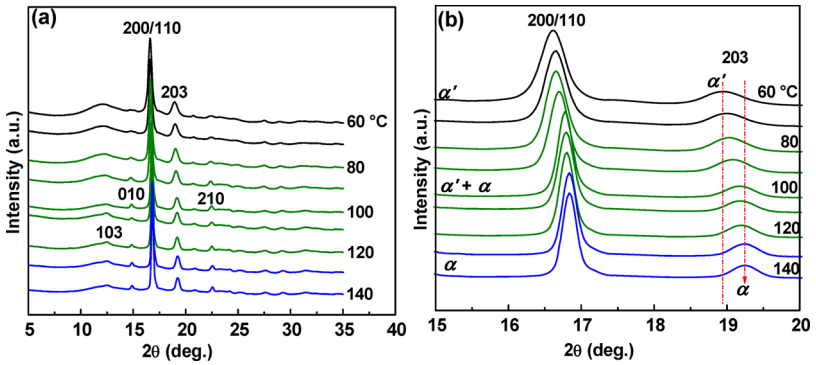

Figure 10. WAXS patterns measured at room temperature for PLLA-*b*-PDMS-*b*-PLLA triblock copolymers crystallized at various cold crystallization temperatures.

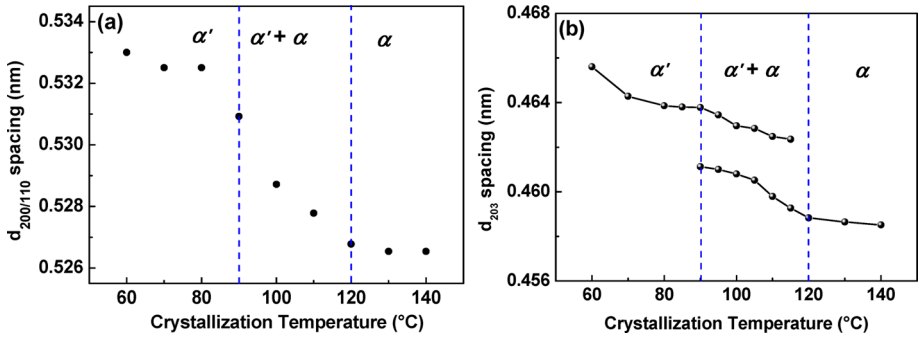

Figure 11. The *d*-spacing values estimated from (a) 200/110 and (b) 203 reflections of PLLA (triblock copolymer) crystallized at various cold crystallization temperatures.

this temperature range. At this temperature, the molten PDMS chains, which are confined within the PLLA microdomains, were stretched as a result of segmental mobility of the PLLA chains. This situation might have resulted in the increase of PDMS microdomain thickness. On the other hand, the microdomain thickness of the PLLA has increased because of the formation of mesophase PLLA in the triblock copolymer just above the glass transition temperature. On further heating, the PLLA block crystallized in a broad temperature range from 80 to 120 °C. At this temperature, the PDMS block is in the molten state, and as a result, the morphological perturbation was induced by the breakout crystallization of PLLA block (Figure 9d). Above the melting of PLLA, both the PDMS and PLLA chains exhibited the random coiled chain conformations with the long period value of 26.4 nm similar to the amorphous PLLA-*b*-PDMS-*b*-PLLA triblock copolymer (Figure 9e).

Polymorphic Behavior of PLLA in PLLA-*b*-PDMS-*b*-PLLA Triblock Copolymer. As mentioned in the preceding section, it has been reported that the polymorphic crystalline forms of PLLA are related to the crystallization temperature. The critical crystallization temperature for the formation of pure α form in PLLA homopolymer is 120 °C.[13−15] It was reported that the polymorphism of PLLA is not influenced much by the molecular weight of the PLLA homopolymer, and the critical crystallization temperature for the formation of pure α form remains at 120 °C, despite the molecular weight.[13] However, it has been reported that the critical crystallization temperature for the formation of pure α form can be reduced to lower crystallization temperature ∼80 °C by miscible blending of PLLA with PDLLA or by reducing the glass transition temperature of PLLA using plasticizers.[68,69] Despite the extensive studies on the polymorphic behavior of PLLA homopolymer, little attention has been paid to understand the polymorphic behavior of PLLA in block copolymers.[22] It is worth mentioning here that most of the previous studies have been used the melt-crystallized samples to understand the effect of crystallization temperatures on the polymorphic behavior of PLLA. In this study, the effect of cold crystallization temperatures (T_{cc}) on the polymorphic behavior of PLLA in PLLA-*b*-PDMS-*b*-PLLA triblock copolymer was systematically investigated by WAXS, SAXS, and FTIR.

Amorphous PLLA-*b*-PDMS-*b*-PLLA triblock copolymer was prepared by cooling the melt to room temperature at a rate of 50 °C/min. Such amorphous sample was reheated to a desired crystallization temperature at a rate of 100 °C/min and kept it for 1 h for the isothermal crystallization. Figure 10 shows the WAXS patterns of the samples crystallized at various temperatures from the amorphous PLLA-*b*-PDMS-*b*-PLLA triblock copolymer. Notable differences in the WAXS patterns are observed between the samples crystallized at low and high crystallization temperatures. The two strong reflections are observed at 2θ = 16.6° and 19.0°, which have been assigned to the reflections of 200/110 and 203 planes (Figure 10b).[13,14] A careful observation of these patterns showed two significant differences. The position of 200/110 reflection shifts to higher 2θ with the crystallization temperature. Figure 11a shows the variation of *d*-spacings of 200/110 reflection against the T_{cc}. The *d*-spacing of samples crystallized below 90 °C is constant, and these values are in good agreement with the α' form. The *d*-spacing of samples crystallized above 120 °C is also constant with a different value, and it is in good agreement with the α form, whereas the samples crystallized in between these crystallization temperatures showed variation in the *d*-spacing with the T_{cc} indicating the presence of both α' and α forms. On

DOI: 10.1021/acs.macromol.5b01179
Macromolecules 2015, 48, 5367−5377

the other hand, the 203 reflection can be resolved into two peaks originating from the α' and α forms for the samples crystallized in between 90 and 120 °C as shown in Figure 11b.[15] Apart from these observations, as reported in the literature, a few more changes were also observed in the different 2θ region between the samples crystallized at low and high crystallization temperatures.[13−15,68−70] The samples crystallized at lower T_{cc} showed a weaker reflection at 2θ = 24.6°, which is a characteristic reflection of the α' form. This reflection disappeared at higher crystallization temperatures above 120 °C. The samples crystallized higher T_{cc} show some additional small reflections at 2θ = 12.5°, 15.0°, 20.7°, 24.1°, 25.1°, and 31.5°, which have been assigned to the characteristic reflections of the α form.

For getting more insight about the polymorphic crystalline forms of PLLA, FTIR measurements were carried out for the amorphous PLLA-*b*-PDMS-*b*-PLLA triblock copolymer samples crystallized at various temperatures. As reported in the literature, the C═O stretching band region 1700−1850 cm^{-1} can be used to distinguish between the α' and α crystalline forms.[13,16,65,71] Figure 12 shows the FTIR spectra of the C═O

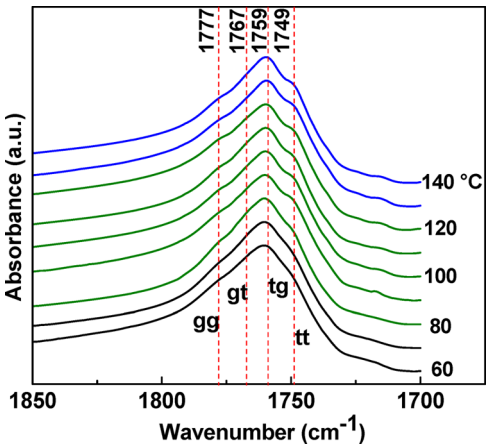

Figure 12. FTIR spectra measured at room temperature for PLLA-*b*-PDMS-*b*-PLLA triblock copolymers crystallized at various cold crystallization temperatures in the frequency region 1700−1850 cm^{-1}.

stretching band region for the amorphous PLLA-*b*-PDMS-*b*-PLLA triblock copolymer samples crystallized at various temperatures. As the cold crystallization temperature increases from 60 to 140 °C, in addition to the band at 1759 cm^{-1}, three new bands are appeared above 90 °C at 1749, 1768, and 1776 cm^{-1}, indicating the structural phase transition from α' to α form. The absence of these bands (1749, 1768, and 1776 cm^{-1}) at lower crystallization temperatures is due to the weak intermolecular interactions and disordered chain packing in the crystallites of the α' form. At higher crystallization temperatures above 90 °C, ordered chain packing occurs due to the rearrangement of molecular chains, and as a result, stronger intermolecular interactions takes place in the crystal lattice to form more stable α form. On the basis of these results, we may say that the α'-to-α transition temperature of PLLA-*b*-PDMS-*b*-PLLA triblock copolymer is not influenced much by the presence of PDMS blocks.

CONCLUSIONS

In this work, we investigated the breakout and preservation of the nanostructure morphology during heating of the amorphous PLLA-*b*-PDMS-*b*-PLLA triblock copolymer by variable temperature small-angle and wide-angle X-ray scattering (SAXS and WAXS). On the basis of the experimental results, we found that the crystallization and melting of PDMS did not alter the dimensions of the microphase-separated domains. At this temperature, the amorphous PLLA created a robust template similar to hard confinement for the PDMS crystallization and melting. However, at around the glass transition temperature of PLLA (∼45 °C), a sudden increase in the microdomain thickness was observed due to the chain stretching of PLLA and PDMS. In this temperature range, the PLLA in triblock copolymer was transiently transformed to the mesophase before transforming into the stable α crystalline form. At higher temperature, the morphological perturbation was induced by the breakout crystallization of PLLA. We believe that the present results provide some new insights into the mechanism of the structure and morphology formation during the heating process of crystallizable block copolymers. In addition, the polymorphic behavior of PLLA in PLLA-*b*-PDMS-*b*-PLLA triblock copolymers was investigated. The critical crystallization temperature for the formation of α' and α forms of PLLA in PLLA-*b*-PDMS-*b*-PLLA triblock copolymer remains the same as the PLLA homopolymer.

ASSOCIATED CONTENT

Supporting Information

Figure S1: DSC temperature program used for the isothermal crystallization of PLLA in poly(L-lactide-*b*-dimethylsiloxane-*b*-L-lactide) triblock copolymer; Figure S2: ^{1}H NMR of poly(L-lactide-*b*-dimethylsiloxane-*b*-L-lactide) triblock copolymer; the transition temperatures of PDMS were evaluated using variable temperature wide-angle X-ray diffraction; Figure S3: (a) WAXS patterns of PDMS homopolymer as a function of temperature upon heating (b) temperature dependence of the integrated intensity of 011 reflection; details about the one-dimensional electron density correlation function ($K(z)$). The Supporting Information is available free of charge on the ACS Publications website at DOI: 10.1021/acs.macromol.5b01179.

AUTHOR INFORMATION

Corresponding Author

*E-mail bhojegowd@niist.res.in; Tel +91-471-2515474; Fax +91-471-2491712 (E.B.G.).

Notes

The authors declare no competing financial interest.

ACKNOWLEDGMENTS

The authors thank Dr. Suresh Das for his constant support and encouragement. S.N. is grateful to CSIR, New Delhi, for the Research Associate Fellowship. E.B.G. thanks the Department of Science and Technology (Government of India) for the award of Ramanujan fellowship and also the financial support from Council of Scientific and Industrial Research, Government of India, under network project CSC-0114.

DEDICATION

This paper is dedicated to Dr. Suresh Das on the occasion of his 60th birthday.

REFERENCES

(1) Garlotta, D. *J. Polym. Environ.* **2001**, *9*, 63−84.

DOI: 10.1021/acs.macromol.5b01179
Macromolecules 2015, 48, 5367−5377

(2) Lim, L. T.; Auras, R.; Rubino, M. *Prog. Polym. Sci.* **2008**, *33*, 820−852.
(3) Saeidlou, S.; Huneault, M. A.; Li, H.; Park, C. B. *Prog. Polym. Sci.* **2012**, *37*, 1657−1677.
(4) Liu, G.; Zhang, X.; Wang, D. *Adv. Mater.* **2014**, *26*, 6905−6911.
(5) Lasprilla, A. J. R.; Martinez, G. A. R.; Lunelli, B. H.; Jardini, A. L.; Filho, R. M. *Biotechnol. Adv.* **2012**, *30*, 321−328.
(6) Zhu, K. J.; Xiangzhou, L.; Shilin, Y. *J. Appl. Polym. Sci.* **1990**, *39*, 1−9.
(7) Fambri, L.; Pegoretti, A.; Fenner, R.; Incardona, S. D.; Migliaresi, C. *Polymer* **1997**, *38*, 79−85.
(8) Leenslag, J. W.; Pennings, A. J.; Bos, R. R. M.; Rozema, F. R.; Boering, G. *Biomaterials* **1987**, *8*, 70−73.
(9) Hoogsteen, W.; Postema, A. R.; Pennings, A. J.; Ten Brinke, G.; Zugenmaier, P. *Macromolecules* **1990**, *23*, 634−642.
(10) Puiggali, J.; Ikada, Y.; Tsuji, H.; Cartier, L.; Okihara, T.; Lotz, B. *Polymer* **2000**, *41*, 8921−8930.
(11) Cartier, L.; Okihara, T.; Ikada, Y.; Tsuji, H.; Puiggali, J.; Lotz, B. *Polymer* **2000**, *41*, 8909−8919.
(12) Marubayashi, H.; Asai, S.; Sumita, M. *Macromolecules* **2012**, *45*, 1384−1397.
(13) Pan, P.; Kai, W.; Zhu, B.; Dong, T.; Inoue, Y. *Macromolecules* **2007**, *40*, 6898−6905.
(14) Kawai, T.; Rahman, N.; Matsuba, G.; Nishida, K.; Kanaya, T.; Nakano, M.; Okamoto, H.; Kawada, J.; Usuki, A.; Honma, N.; Nakajima, K.; Matsuda, M. *Macromolecules* **2007**, *40*, 9463−9469.
(15) Zhang, J.; Tashiro, K.; Tsuji, H.; Domb, A. J. *Macromolecules* **2008**, *41*, 1352−1357.
(16) Zhang, J.; Duan, Y.; Sato, H.; Tsuji, H.; Noda, I.; Yan, S.; Ozaki, Y. *Macromolecules* **2005**, *38*, 8012−8021.
(17) Sasaki, S.; Asakura, T. *Macromolecules* **2003**, *36*, 8385−8390.
(18) Wasanasuk, K.; Tashiro, K.; Hanesaka, M.; Ohhara, T.; Kurihara, K.; Kuroki, R.; Tamada, T.; Ozeki, T.; Kanamoto, T. *Macromolecules* **2011**, *44*, 6441−6452.
(19) Marubayashi, H.; Asai, S.; Sumita, M. *J. Phys. Chem. B* **2013**, *117*, 385−397.
(20) Sawai, D.; Yokoyama, T.; Kanamoto, T.; Sungil, M.; Hyon, S.-H.; Myasnikova, L. P. *Macromol. Symp.* **2006**, *242*, 93−103.
(21) Cocca, M.; Lorenzo, M. L. D.; Malinconico, M.; Frezza, V. *Eur. Polym. J.* **2011**, *47*, 1073−1080.
(22) Ho, C.-H.; Jang, G.-W.; Lee, Y.-D. *Polymer* **2010**, *51*, 1639−1647.
(23) Hobbs, R. G.; Farrell, R. A.; Bolger, C. T.; Kelly, R. A.; Morris, M. A.; Petkov, N.; Holmes, J. D. *ACS Appl. Mater. Interfaces* **2012**, *4*, 4637−4642.
(24) Castillo, R. V.; Müller, A. J. *Prog. Polym. Sci.* **2009**, *34*, 516−560.
(25) Voet, V. S. D.; Alberda van Ekenstein, G. O. R.; Meereboer, N. L.; Hofman, A. H.; Brinke, G. t.; Loos, K. *Polym. Chem.* **2014**, *5*, 2219−2230.
(26) Rodwogin, M. D.; Spanjers, C. S.; Leighton, C.; Hillmyer, M. A. *ACS Nano* **2010**, *4*, 725−732.
(27) Zhang, S.; Hou, Z.; Gonsalves, K. E. *J. Polym. Sci., Part A: Polym. Chem.* **1996**, *34*, 2737−2742.
(28) Jung, Y. S.; Ross, C. A. *Adv. Mater.* **2009**, *21*, 2540−2545.
(29) Hamley, I. W. Introduction to Block Copolymers. In *Developments in Block Copolymer Science and Technology*; John Wiley & Sons, Ltd: New York, 2004; pp 1−29.
(30) Müller, A.; Balsamo, V.; Arnal, M. Nucleation and Crystallization in Diblock and Triblock Copolymers. In *Block Copolymers II*; Abetz, V., Ed.; Springer: Berlin, 2005; Vol. *190*, pp 1−63.
(31) Nandan, B.; Hsu, J. Y.; Chen, H. L. *J. Macromol. Sci., Polym. Rev.* **2006**, *46*, 143−172.
(32) Ryan, A. J.; Fairclough, J. P. A.; Hamley, I. W.; Mai, S.-M.; Booth, C. *Macromolecules* **1997**, *30*, 1723−1727.
(33) Ryan, A. J.; Hamley, I. W.; Bras, W.; Bates, F. S. *Macromolecules* **1995**, *28*, 3860−3868.
(34) Hamley, I. W. Crystallization in Block Copolymers. In *Interfaces Crystallization Viscoelasticity*; Springer: Berlin, 1999; Vol. *148*, pp 113−137.
(35) He, W.-N.; Xu, J.-T. *Prog. Polym. Sci.* **2012**, *37*, 1350−1400.
(36) Loo, Y.-L.; Register, R. A.; Ryan, A. J. *Macromolecules* **2002**, *35*, 2365−2374.
(37) Zhu, L.; Cheng, S. Z. D.; Calhoun, B. H.; Ge, Q.; Quirk, R. P.; Thomas, E. L.; Hsiao, B. S.; Yeh, F.; Lotz, B. *Polymer* **2001**, *42*, 5829−5839.
(38) Douzinas, K. C.; Cohen, R. E. *Macromolecules* **1992**, *25*, 5030−5035.
(39) Cohen, R. E.; Bellare, A.; Drzewinski, M. A. *Macromolecules* **1994**, *27*, 2321−2323.
(40) Hamley, I. W.; Fairclough, J. P. A.; Terrill, N. J.; Ryan, A. J.; Lipic, P. M.; Bates, F. S.; Towns-Andrews, E. *Macromolecules* **1996**, *29*, 8835−8843.
(41) Rangarajan, P.; Register, R. A.; Fetters, L. J. *Macromolecules* **1993**, *26*, 4640−4645.
(42) Voet, V. S. D.; Tichelaar, M.; Tanase, S.; Mittelmeijer-Hazeleger, M. C.; ten Brinke, G.; Loos, K. *Nanoscale* **2013**, *5*, 184−192.
(43) Müller, A.; Arnal, M.; Balsamo, V. Crystallization in Block Copolymers with More than One Crystallizable Block. In *Progress in Understanding of Polymer Crystallization*; Reiter, G., Strobl, G., Eds.; Springer: Berlin, 2007; Vol. *714*, pp 229−259.
(44) Chiang, Y.-W.; Huang, Y.-W.; Huang, S.-H.; Huang, P.-S.; Mao, Y.-C.; Tsai, C.-K.; Kang, C.-S.; Tasi, J.-C.; Su, C.-J.; Jeng, U. S.; Tseng, W.-H. *J. Phys. Chem. C* **2014**, *118*, 19402−19414.
(45) He, C.; Sun, J.; Deng, C.; Zhao, T.; Deng, M.; Chen, X.; Jing, X. *Biomacromolecules* **2004**, *5*, 2042−2047.
(46) He, C.; Sun, J.; Ma, J.; Chen, X.; Jing, X. *Biomacromolecules* **2006**, *7*, 3482−3489.
(47) Hamley, I. W.; Castelletto, V.; Castillo, R. V.; Müller, A. J.; Martin, C. M.; Pollet, E.; Dubois, P. *Macromolecules* **2005**, *38*, 463−472.
(48) Sun, J.; Hong, Z.; Yang, L.; Tang, Z.; Chen, X.; Jing, X. *Polymer* **2004**, *45*, 5969−5977.
(49) Castillo, R. V.; Müller, A. J.; Raquez, J.-M.; Dubois, P. *Macromolecules* **2010**, *43*, 4149−4160.
(50) Yang, J.; Liang, Y.; Luo, J.; Zhao, C.; Han, C. C. *Macromolecules* **2012**, *45*, 4254−4261.
(51) Lin, M.-C.; Chen, H.-L.; Su, W.-B.; Su, C.-J.; Jeng, U. S.; Tzeng, F.-Y.; Wu, J.-Y.; Tsai, J.-C.; Hashimoto, T. *Macromolecules* **2012**, *45*, 5114−5127.
(52) Li, S.; Myers, S. B.; Register, R. A. *Macromolecules* **2011**, *44*, 8835−8844.
(53) Castillo, R. V.; Arnal, M. L.; Müller, A. J.; Hamley, I. W.; Castelletto, V.; Schmalz, H.; Abetz, V. *Macromolecules* **2008**, *41*, 879−889.
(54) Nojima, S.; Akutsu, Y.; Washino, A.; Tanimoto, S. *Polymer* **2004**, *45*, 7317−7324.
(55) Nojima, S.; Akutsu, Y.; Akaba, M.; Tanimoto, S. *Polymer* **2005**, *46*, 4060−4067.
(56) Castillo, R. V.; Müller, A. J.; Lin, M.-C.; Chen, H.-L.; Jeng, U. S.; Hillmyer, M. A. *Macromolecules* **2008**, *41*, 6154−6164.
(57) Lund, R.; Alegría, A.; Goitandía, L.; Colmenero, J.; González, M. A.; Lindner, P. *Macromolecules* **2008**, *41*, 1364−1376.
(58) Dollase, T.; Spiess, H. W.; Gottlieb, M.; Yerushalmi-Rozen, R. *J. Macromol. Sci., Pure Appl. Chem.* **2002**, *60*, 390.
(59) Dollase, T.; Wilhelm, M.; Spiess, H. W.; Yagen, Y.; Yerushalmi-Rozen, R.; Gottlieb, M. *Interface Sci.* **2003**, *11*, 199−209.
(60) Strobl, G. R.; Schneider, M. J. *J. Polym. Sci., Polym. Phys. Ed.* **1980**, *18*, 1343−1359.
(61) Gowd, E. B.; Shibayama, N.; Tashiro, K. *Macromolecules* **2008**, *41*, 2541−2547.
(62) Goderis, B.; Reynaers, H.; Koch, M. H. J.; Mathot, V. B. F. *J. Polym. Sci., Part B: Polym. Phys.* **1999**, *37*, 1715−1738.

DOI: 10.1021/acs.macromol.5b01179
Macromolecules 2015, 48, 5367−5377

(63) Shi, W.; McGrath, A. J.; Li, Y.; Lynd, N. A.; Hawker, C. J.; Fredrickson, G. H.; Kramer, E. J. *Macromolecules* **2015**, *48*, 3069−3079.
(64) Meaurio, E.; Martinez de Arenaza, I.; Lizundia, E.; Sarasua, J. R. *Macromolecules* **2009**, *42*, 5717−5727.
(65) Meaurio, E.; Zuza, E.; López-Rodríguez, N.; Sarasua, J. R. *J. Phys. Chem. B* **2006**, *110*, 5790−5800.
(66) Zhang, J.; Duan, Y.; Domb, A. J.; Ozaki, Y. *Macromolecules* **2010**, *43*, 4240−4246.
(67) Albuerne, J.; Márquez, L.; Müller, A. J.; Raquez, J. M.; Degée, P.; Dubois, P.; Castelletto, V.; Hamley, I. W. *Macromolecules* **2003**, *36*, 1633−1644.
(68) Pan, P.; Liang, Z.; Zhu, B.; Dong, T.; Inoue, Y. *Macromolecules* **2009**, *42*, 3374−3380.
(69) Koido, S.; Kawai, T.; Kuroda, S.; Nishida, K.; Kanaya, T.; Kato, M.; Kurose, T.; Nakajima, K. *J. Appl. Polym. Sci.* **2014**, *131*, 39762-1−39762-8.
(70) Pan, P.; Zhu, B.; Kai, W.; Dong, T.; Inoue, Y. *Macromolecules* **2008**, *41*, 4296−4304.
(71) Meaurio, E.; López-Rodríguez, N.; Sarasua, J. R. *Macromolecules* **2006**, *39*, 9291−9301.

DOI: 10.1021/acs.macromol.5b01179
Macromolecules 2015, 48, 5367−5377